Anomalies in the fission yields of light actinides explained by memory effects in nuclear dynamics

Karl-Heinz Schmidt [1a], *Christelle* Schmitt[2,3], and *Andreas* Heinz[4]

[1]Independent researcher, 64390 Erzhausen, Germany
[2]Institut Pluridisciplinaire Hubert Curien, CNRS/IN2P3-UDS, 67037 Strasbourg Cedex 2, France
[3]Institute of Nuclear Physics Polish Academy fo Sciences, 31-342 Krakow, Poland
[4]Department of Physics, Chalmers University of Technology, 41296 Gothenburg, Sweden

Abstract. Already in the 1970ies, deviations in fission excitation functions and fragment angular anisotropies from the trend established for heavier systems were observed in the fission of light actinides. This was referred to as the "thorium anomaly", and it was interpreted in terms of the occurrence of a triple-humped fission barrier. In this contribution we demonstrate that also the fragment yields from the fission of these nuclei show abnormal features, which have been overlooked up to now. The analysis of these observables, and of their variation as a function of the initial excitation energy *E** reveals the suppression of compact shapes at scission for E* below a certain threshold. Our findings provide new insight into the transport properties of nuclear matter, like inertial mass and viscosity. Our results are in severe conflict with the widely used assumption that the role of collective inertia in fission dynamics is negligible. They falsify the validity of approaches disregarding the influence of inertia, like statistical scission-point models or the use of the Smoluchowsky equation in stochastic approaches.

1 Introduction

Since its discovery [1,2] , the research on nuclear fission has brought important progress on the general understanding of static and dynamic properties of nuclei. The unexpectedly low threshold of nuclear fission due to the complex shape evolution triggered the study of large-scale collective motion [3] . The dominance of asymmetric fission of actinide nuclei at low excitation energies stimulated the development of the nuclear shell model [4,5] .The discovery of shape isomers [6} revealed the oscillatory behaviour of shell effects as a function of shape distortions. The observation of pre-scission neutrons [7] initiated intense efforts for determining the transport properties of nuclear matter like viscosity and inertial mass. Still, there is urgent need for high-quality fission data that constrain the dissipation tensor [8] .

This work aims at meeting this demand by compiling, analysing and interpreting various data that are directly related to the transport properties of nuclear matter. Section 2 of this contribution consists of four parts which build up one upon the other. Section 2.1 demonstrates and discusses the reasons for a broad systematic behaviour of the fission yields that appears for almost all fissioning systems. In Section 2.2, we work out local deviations, appearing in the fission of light actinides, and we extract the common features and the characteristics of these deviations. In Section 2.3, we illuminate the striking similarities of the deviations in the yields and the often postulated appearance of a third minimum in the fission barrier. In Section 2.4, we interpret the observed deviations in the fission yields in terms of relaxation effects in mass-asymmetric distortions. Finally, in Section 3, we discuss the implications of our analysis for the underlying transport properties of nuclear matter.

a Corresponding author: schmidt-erzhausen@t-online.de

2 Manifestation and interpretation of anomalies in the fission yields

This work emerged as a by-product of the GEF model [9] . In the development of GEF, it was the paramount interest to find a simple but powerful description of the fission process. For this purpose, the search for systematic tendencies in the data, eventually combined with theoretical arguments was a mandatory process. On this occasion, the systematics that will be described in Section 2.1 and the anomalies that will be shown in Section 2.2 became evident. Here, we give only a concise summary. For a detailed description, we refer to Ref. [9]. Similarities in the appearance of the "thorium anomaly" and the observed anomalies in the fission yields are addressed in Section 2.3. An interpretation of the excitation-energy dependence of the anomalies is given in Section 2.4. These results form the basis for the new insights in the transport properties of nuclear matter, postulated in Section 3.

2.1 Systematics of fission yields

One of the most powerful ingredients of GEF is the separability principle [10] . It is based on the early result of calculations with the two-centre shell model [11] . According to these calculations, the single-particle levels show patterns of shell structure already for shapes slightly beyond the second saddle that resemble those of the separated fragments. This means that the structures in the potential energy are essentially determined by the fragments, and only the macroscopic potential energy depends on the fissioning system. This kind of separability holds also for the fission yields, because in GEF the yields are determined by the phase space for a certain mass-asymmetric distortion. Thus, the separability principle means that the structural effects in the fission yields are attributed to the fragments, and the influence of the fissioning nucleus is limited to the macroscopic (smooth) contribution.

In this way, the almost constant mass A=140 or nuclear charge Z=54 of the heavy component of asymmetric fission in the actinides [12,13] can be explained. Figure 3 of Ref. [14] shows that this simple recipe empowers GEF to reproduce the measured mass distributions for a large variety of fissioning nuclei rather closely.

2.2 Anomalies

A thorough analysis shows that the global systematics from Fig. 3 of [14] is broken for a number of fissioning nuclei in the light actinides. As an example, a drastic deviation is seen in Fig. 1 for the fragment mass distribution of ^{238}U(sf). Unfortunately, the ENDF evaluation contains only data for spontaneous fission and fission induced by neutrons with thermal or fast neutrons (below 2 MeV) and 14-MeV neutrons.

An attempt to determine the fission-channel yields as a function of excitation energy in detail was made by Brosa et al. [15]. For compound nuclei ranging from ^{232}Th to ^{242}Pu, endowed with excitation energies typically between 0 and 10 MeV, they analysed variations of the fission-fragment mass distributions in terms of a fission-channel model [16]. The study was based on previously measured pre-neutron mass distributions and, partly, total kinetic energies (*TKE*) with a typical resolution of about 4 masses. Although the extraction of the fission-channel yields, performed by Brosa et al. [15], suffered from limitations due to poor mass resolution and statistics, and from a dependence on the fitting method, two unequivocal results were obtained: (i) In the energy range investigated, the yield of the S1 fission channel grows on the average for fissioning nuclei below A = 235, while it decreases for heavier nuclei with increasing initial excitation energy (see Fig. 4 in Ref. [15]). (ii) The result for the compound nucleus ^{236}U, based on high-statistics data and performed with a two-dimensional (A-TKE) fit, shows an inversion of the slope at an excitation energy of E^* = 8 MeV, see Fig. 2.

There exist a few more data that are affected by similar anomalies as those of Figs. 1 and 2. They cannot be shown here due to space restrictions. Considering all available data, the anomaly consists of reduced fission yields with heavy fragments around Z=50 for energies below a threshold that depends on the fissioning nucleus. The threshold increases towards lower Z values of the fissioning nucleus.

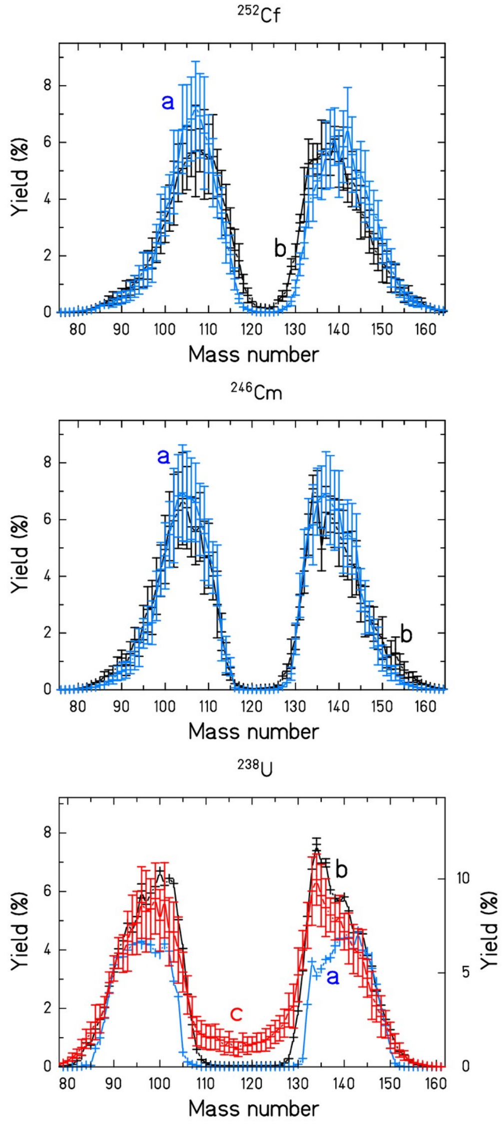

Fig. 1. Illustration of the anomalous shape of the asymmetric peaks in the mass distribution from spontaneous fission of ^{238}U. Blue symbols (a): spontaneous fission, black symbols (b): fission induced by neutrons below 2 MeV, red symbols (c): fission induced by 14-MeV neutrons (fully resolved mass yields after prompt-neutron emission from ENDF/B-VII [17]). (In some cases, the data from nearby nuclei are shown, due to the lack of available data, see Table 1.) The distribution from spontaneous fission of ^{238}U was scaled to fit to the yields from fission induced by low-energy neutrons in the outer part of the light asymmetric peak around mass 90 (see right scale). This illustrates that the anomaly in ^{238}U(sf) can be understood as caused by a suppression of the inner parts of the asymmetric peaks of ^{238}U(sf) in comparison with all other mass distributions shown in the figure. All data refer to the masses after prompt-neutron emission.

Based on all available data, an empirical description of these anomalies is implemented in GEF-Y2025/V1.1 and in more recent versions. The impact of these anomalies on nuclear technology was already pointed out in a dedicated publication[18}.

Table 1. List of fissioning system used in figure 1.

Nominal system	Spontaneous fission	Low-energy neutrons	High-energy neutrons
^{238}U	^{238}U(sf)	^{238}U(n,f), $E_n \approx 2$ MeV	^{238}U(n,f), $E_n \approx 14$ MeV
^{246}Cm	^{246}Cm(sf)	^{245}Cm(n_{th},f)	No data available
^{250}Cf	^{252}Cf(sf)	^{249}Cf(n_{th},f)	No data available

Due to the lack of measured fission yields, in some cases, the values of the nominal systems at the excitation energies of interest are not available. The mass yields from nearby systems are shown in these cases in Fig. 1. This choice does not have any sizeable influence on the conclusions of the present work, because the measured yields of fissioning nuclei in the region of those, which are of interest for our analysis, are generally found to be composed of the same fission channels with smoothly varying probabilities as a function of *Z* and *A* [14]. The differences of the yields of neighbouring fissioning isotopes generally do hardly exceed the experimental uncertainties.

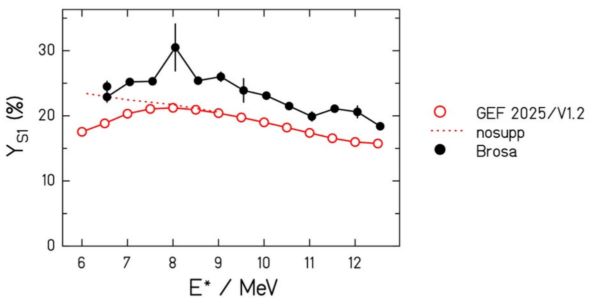

Fig 2. Variation of the yield of the S1 fission channel as a function of the excitation energy in the fission of the compound nucleus ^{236}U. The values from Ref. [15] (full symbols) show the same trend with a maximum at 8 MeV as the result of GEF-2025/V1.2 (open symbols). The dotted line shows the GEF result without the influence of the 3rd barrier.

2.3 Relation with the appearance of a third minimum

The fact that the anomalies in the fission yields appear in the lighter actinides and disappear for nuclei beyond uranium reminds of an anomaly that was observed in the 1970's in the fission excitation functions of several thorium isotopes [19] and attributed to the presence of a third minimum in the fission barrier [20]. It is tempting to assume that both types of anomalies have the same origin, namely the presence of a third minimum, which implies also the presence of a third barrier.

Figure 3 shows a schematic drawing of the potential along the fission path. The values marked by a symbol are deduced from measured or evaluated data. The lines are splines, only for guiding the eye. The potential beyond the second barrier is a rough estimate on the basis of the value of E_B-E_A. The reason for the increase of this value for lighter nuclei is the broadening of the macroscopic barrier, see Fig. 4 in Ref. [21].

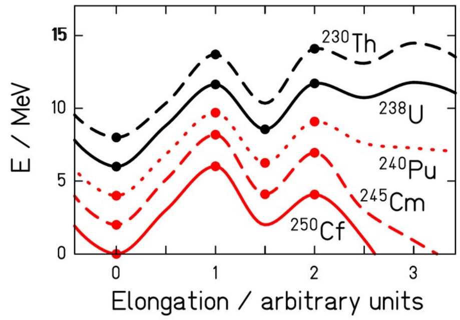

Fig. 3. Schematic drawing of the potential energy along the fission path. The curves for *Z*<98 are displaced by ΔE = (98-*Z*) MeV for better visibility. The drawing is based on empirical values (marked by data points) of the heights of the first and the second barrier above the ground state (elongation = 0) as well as of the depth of the second minimum. The oscillations that form the multi-humped fission barrier are very similar, while the large-scale (or macroscopic) behaviour that is described by the nuclear liquid-drop model shows a trend from a broad barrier in ^{230}Th to an appreciably narrower one in ^{250}Cf. This trend leads to the appearance of a third barrier with comparable height to the first and the second barrier in the lighter systems. The figure is stimulated by Fig. 4 in Ref. [21], where also the trend of the macroscopic barrier is explicitly shown.

2.4 Interpretation

We propose the following scenario as an explanation for the observed anomalies in the fission yields : For mass splits with heavy fragments around tin it is known that the *TKE* exploits almost the total Q value. In this case, it is possible that the third barrier cannot be passed without tunneling at low initial excitation energy. This leads to a suppression of the yield. The presence of a threshold energy and the increasing suppression at lower initial excitation energy reminds the typical characteristic of a tunneling process.

The disappearance of the suppression effect above the threshold energy is a strong indication that the mass-asymmetric distortion, established at the second barrier, is preserved up to scission, if the initial excitation energy is high enough that the third barrier can be passed without tunneling. Thus, the excitation-energy dependent suppression effect carries pre-eminent information on the dynamic properties of nuclear matter. A detailed discussion of this finding in terms of a stochastic description of the fission process will be given in the next section.

3 Implications for the nuclear transport properties

Multi-dimensional Langevin dynamics is a well established approach for the description of large-scale collective motion of nuclei like fission [22]. In contrast to a fully microscopic description, based on the the forces that act between any nucleon with all the others, only the collective degrees of freedom are explicitly considered, while the bulk of intrinsic degrees of freedom are represented by a medium, characterized by a few global parameters like temperature and viscosity. The classical Langevin equation for an object in one dimension reads:

$$m\, \mathrm{d}/\mathrm{d}t\, (v(t)) = F(x) - \xi v(\mathrm{t}) + f(t) \qquad (1)$$

The driving force $F(x)$, the friction force $\xi v(\mathrm{t})$ and the random force $f(t)$ act on the motion of the object with mass m and induce a variation of its velocity v. m d/dt(v(t)) is the inertial force, connected with the acceleration or deceleration of the object. The driving force is given be

$$F(x) = T\, \mathrm{d}S/\mathrm{d}x, \qquad ..(2)$$

with T = temperature and S = entropy as given by the state density of the system [23]. It depends on excitation energy and on the shape of the system under the condition of a constant total energy. The driving force represents the influence of the shape-dependent potential energy. The friction is assumed here to be a Stokes force that is proportional to the velocity v of the system. Its strength is determined by the friction coefficient ξ that is connected with the viscosity of the environment. Viscosity has an intimate connection with the random force $f(t)$, which is expressed by the Einstein relation. The magnitude of inertia and dissipation is given by their respective transport coefficient. The inertial mass and the dissipation coefficients may depend on the specific kind of shape distortion, the value of the corresponding distortion as well as on temperature and other parameters.

In the present context, the motion in two dimensions is in the centre of interest: The evolution of mass-asymmetric distortions along the fission path, which is represented by an elongation parameter. This problem has carefully been investigated in Ref. [24] by use of the Fokker-Planck equation, which is equivalent to the Langevin equation.

The memory of the mass-asymmetric distortion beyond the second barrier, deduced from the energy-dependent anomalies, indicates that the corresponding relaxation time is longer than the time needed to move from the second barrier to scission. As discussed in Ref [24], the relaxation time depends on the magnitudes of inertial mass and dissipation. Both, large inertial mass combined with weak dissipation and large dissipation with small inertial mass lead to long relaxation times. In Ref. [24], it is argued that the inertial mass increases especially strongly with increasing elongation, which is accompanied with a decreasing neck diameter d; towards d=0, it even diverges. This would suggest that the long relaxation time is primarily caused by the inertial mass. Thus, dynamical calculations of the fission process must include the influence of inertial forces. This requirement is not always respected.

The result of an advanced microscopic parameter-free calculation using the TDSLDA (time-dependent super-fluid local density approximation) framework has been interpreted as the first microscopic justification for the assumption that the influence of inertia in fission dynamics is irrelevant [25]. Our results are in conflict with this conclusion, which had been raised already by the authors of the first formulation of the one-body dissipation [26]. They also disprove the validity of the Smoluchowski equation [27] in stochastic approaches to fission or equivalent models that disregards the influence of inertia[28], as well as of statistical scission-point models [29,30,31,32].

A comprehensive quantitative dynamical calculation of fission at low excitation energy, especially when part of the trajectory consists of a tunneling process, challenges current theory. No consistent calculation exists. Sadhukhan and collaborators [33] used an hybrid model for calculating fragment yields. They combined the transmission through a barrier by tunneling with classical Langevin dynamics beyond the saddle. Comparing such kind of calculation with the observed anomalies in the fission yields could help to deduce quantitative conclusions on the transport coefficients of nuclear matter.

4 Conclusion

In accordance with the statement of Nils Bohr that the starting point of knowledge is empirical evidence [34] , we have compiled the manifestations of abnormal yields, appearing in the fission of light actinides, and extracted their common features and general characteristics. On this basis, this work explains these observations in a way that is consistent with related present knowledge. In particular, the similarity of the excitation-energy dependence of the observed anomalies with the Hill-Wheeler formula [35] and the appearance for nuclei that show other signatures of a third fission barrier strongly support our hypothesis. Still missing are the specification of the potential-energy landscape of the fissioning system and the transport properties of nuclear matter, which, however, remain within the uncertainties of present knowledge. It is our hope that our work initiates dedicated studies both in experiment and in theory on this subject.

Acknowledgements

The work was supported by the French-German collaboration between IN2P3-DSM/CEA and GSI, under Agreement No. 19-80. AH is grateful for funding from the Knut and Alice Wallenberg Foundation under KAW 2020.0076.

Author contributions

All authors listed have made a substantial, direct and intellectual contribution to the work.

References

[1] Otto Hahn, Fritz Strassmann, Über den Nachweis und das Verhalten der bei der Bestrahlung des Urans mittels Neutronen entstehenden Erdalkalimetalle. Naturwissenschaften 27, 11 (1939)
[2] Lise Meitner, Otto Robert Frisch, Disintegration of uranium by neutrons: A new type of nuclear reactions. Nature 143, 239 (1939)
[3] N. Bohr, J. A. Wheeler, The mechanism of nuclear fission. Phys. Rev. 56, 426 (1939)
[4] M. Goeppert-Mayer, On closed shells in nuclei. Phys. Rev. 74, 235 (1948)
[5] O. Haxel, J. H. D. Jensen, H. E. Suess, On the 'magic numbers' in nuclear structure. Phys. Rev. 75, 1766 (1949)
[6] S. M. Polikanov, Uspek. Fiz Nauk 94, 43 (1968)
[7] D. Hilscher, H. Rossner, Dynamics of nuclear fission. Ann. Phys. Fr. 17, 471 (1992)
[8] M. Bender et al., Future of nuclear fission theory. J. Phys. G: Nucl. Part. Phys. 47, 113002 (2020)
[9] K.-H. Schmidt, B. Jurado, C. Amouroux, C. Schmitt, General description of fission observables: GEF model code. Nucl. Data Sheets 131, 107 (2016)
[10] K.-H. Schmidt, A. Kelic, M. V. Ricciardi, Experimental evidence for the separability of compound-nucleus and fragment properties in fission. Europh. Lett. 83, 32001 (2008)
[11] U. Mosel, H. W. Schmitt, Fragment-shell influences in nuclear fission. Phys. Rev. C 4, 2185 (1971)
[12] J. P. Unik, J. E. Gindler, L. E. Glendenin, K. F. Flynn, A. Gorski, R. K. Sjoblom, Fragment mass and kinetic energy distributions for fissioning systems ranging from mass 230 to 256, Proc. Symp. Phys. Chem. Fission, Rochester 1973, IAEA Vienna (1974), vol. 2, p. 19
[13] C. Böckstiegel, S. Steinhäuser, K.-H. Schmidt, H.-G. Clerc, A. Grewe, A. Heinz, M. de Jong, A. R. Junghans, J. Müller, B. Voss, Nuclear-fission studies with relativistic secondary beams: analysis of fission channels. Nucl. Phys. A 802, 12 (2008)
[14] K. Mahata, C. Schmitt, Shilpi Gupta, A. Shrivastava, G. Scamps, K.-H. Schmidt, Evidence for the general dominance of proton shells in low-energy fission. Phys. Lett. B 825, 136859 (2022)
[15] U. Brosa, H.-H. Knitter, Tie-shuan Fan, Ji-min Hu, Shang-lian Bao. Systematics of fission-channel probabilities. Phys. Rev. C 59, 767 (1999)
[16] U. Brosa, S. Grossmann, A. Müller. Nuclear scission, Phys. Rep. 197, 167 (1990)
[17] M. B. Chadwick et al., ENDF/B-VII.1 nuclear data for science and technology: cross sections, covariances, fission product yields and decay data. Nucl. Data Sheets 112, 2287 (2011)
[18] K.-H. Schmidt, Ch. Schmitt, A. Heinz, B. Jurado, Identifying and overcoming deficiencies of nuclear data on the fission of light actinides by use of the GEF code. Ann. Nucl. Energy 208, 110784 (2024)
[19] B. B. Back, H. C. Britt, J. D. Garrett, O. Hansen, Subbarrier fission resonances in Th isotopes. Phys. Rev. Lett. 28 , 1707 (1972)
[20] P. G. Thirolf, D. Habs, Spectroscopy in the second and third minimum of actinide nuclei. Prog. Part. Nucl. Phys. 49, 325 (2002)
[21] R. Vandenbosch, Spontaneously fissioning isomers. Ann. Rev. Nucl. Sc. 27, 1 (1977)
[22] K. Mazurek, P. N. Nadtochy, E. G. Ryabov, G. D. Adeev, Fission fragment distributions within dynamical approach. Eur. Phys. J. A 53, 79 (2017)
[23] P. Fröbrich, On the dynamics of fission of hot nuclei. Nucl. Phys. A 787, 170c (2007)
[24] G. D. Adeev, I. I. Gonchar, V. V. Pashkevich, N. I. Pischasov, O. I. Serdyuk, Diffusion Model of the Formation of Fission-Fragment Distributions. Sov. J. Part. Nucl. 19, 529 (1988)
[25] A. Bulgac, S. Jin, I. Stetcu,. Nuclear fission dynamics: past, present, needs, and future. Front. Phys. 8, 63 (2020)
[26] J. Blocki, Y. Borneh, J. R. Nix, J. Randrup, M. Robel, A. J. Sierk, W. J. Swiatecki, One-body dissipation and the super-viscosity of nuclei. Annals of Physics 113, 330 (1978)
[27] S. Chandrasekhar, Stochastic problems in physics and astronomy. Rev. Mod. Phys. 15, 1 (1943)
[28] J. Randrup,P. Möller, Brownian shape motion on five-dimensional potential-energy surfaces: Nuclear fission-fragment mass distributions. Phys. Rev. Lett. 106, 132503 (2011)
[29] B. D. Wilkins, E. P. Steinberg, R. R. Chasman, Scission-point model of nuclear fission based on deformed-shell effects. Phys. Rev. C 14, 1832 (1976)
[30] N. Carjan, F. A. Ivanyuk,Yu. Ts. Oganessian, Pre-scission model predictions of fission fragment mass distributions for super-heavy elements. Nucl. Phys. A 968, 453 (2017)
[31] H. Pasca, A. V. Andreev, G. G. Adamian, N. V. Antonenko, Simultaneous description of charge, mass, total kinetic energy, and neutron multiplicity distributions in fission of Th and U isotopes. Phys. Rev. C 104, 014604 (2021)
[32] J. F. Lemaitre, S. Goriely, S. Hilaire,J.-L. Sida, Fully microscopic scission-point model to predict fission fragment observables. Phys. Rev. C 99, 034612 (2019)
[33] J. Sadhukhan, W. Nazarewicz, N. Schunk, Microscopic modeling of mass and charge distributions in the spontaneous fission of ^{240}Pu. Phys. Rev. C 93, 011304(R) (2016)
[34] P. F. Bortignon, R. A. Broglia, Challenges in the description of the atomic nucleus: unification and interdisciplinarity. Eur. Phys. J. A 52, 64 (2016)
[35] D. L. Hill, J. A. Wheeler, Nuclear constitution and the interpretation of fission phenomena. Phys. Rev. 89, 1102 (1953)